Temperature, pressure, and compositional effects on anomalous or “self” preservation of gas hydrates

Laura A. Stern, Susan Circone, Stephen H. Kirby, and William B. Durham

Abstract: We previously reported on a thermal regime where pure, polycrystalline methane hydrate is preserved metastably in bulk at up to 75 K above its nominal temperature stability limit of 193 K at 0.1 MPa, following rapid release of the sample pore pressure. Large fractions (>50 vol.%) of methane hydrate can be preserved for 2–3 weeks by this method, reflecting the greatly suppressed rates of dissociation that characterize this “anomalous preservation” regime. This behavior contrasts that exhibited by methane hydrate at both colder (193–240 K) and warmer (272–290 K) isothermal test conditions, where dissociation rates increase monotonically with increasing temperature. Here, we report on recent experiments that further investigate the effects of temperature, pressure, and composition on anomalous preservation behavior. All tests conducted on sI methane hydrate yielded self-consistent results that confirm the highly temperature-sensitive but reproducible nature of anomalous preservation behavior. Temperature-stepping experiments conducted between 250 and 268 K corroborate the relative rates measured previously in isothermal preservation tests, and elevated pore-pressure tests showed that, as expected, dissociation rates are further reduced with increasing pressure. Surprisingly, sII methane–ethane hydrate was found to exhibit no comparable preservation effect when rapidly depressurized at 268 K, even though it is thermodynamically stable at higher temperatures and lower pressures than sI methane hydrate. These results, coupled with SEM imaging of quenched sample material from a variety of dissociation tests, strongly support our earlier arguments that ice-“shielding” effects provided by partial dissociation along hydrate grain surfaces do not serve as the primary mechanism for anomalous preservation. The underlying physical-chemistry mechanism(s) of anomalous preservation remains elusive, but appears to be based more on textural or morphological changes within the hydrate material itself, rather than on compositional zoning or ice-rind development.

PACS Nos.: 82.30Lp, 81.40Gh, 81.40Vw, 68.37Hk, 83.80Nb

Résumé : Nous avons déjà rapporté l’existence d’un régime purement thermique où un

Received 17 July 2002. Accepted 14 January 2003. Published on the NRC Research Press Web site at http://cjp.nrc.ca/ on 4 April 2003.

L.A. Stern,[1] S. Circone, and S.H. Kirby. United States Geological Survey, MS/ 977, Menlo Park, CA 94025, U.S.A.
W.B. Durham. U.C. Lawrence Livermore National Laboratory, Livermore, CA 94550, U.S.A.

[1] Corresponding author (e-mail: lstern@usgs.gov).

Can. J. Phys. **81**: 271–283 (2003) doi: 10.1139/P03-018

hydrate de méthane polycristallin pur est préservé en volume de façon métastable jusqu'à 75 K au dessus de sa température nominale de stabilité, qui est 193 K à 0,1 Mpa, suivant un relâchement rapide de la pression sur les pores du système. On peut conserver de cette façon de larges fractions de l'hydrate (>50% en volume) pendant 2–3 semaines, reflétant la suppression importante des taux de décomposition qui caractérise ce régime « anomal de conservation ». Ce comportement contraste avec les hydrates de méthane dans les conditions isothermes de test à la fois plus froides (193–240 K) et plus chaudes (272–290 K), où les taux de dissociation augmentent de façon monotone avec la température. Nous rapportons ici nos plus récents résultats sur les effets de la température, de la pression et de la composition sur cette conservation anomale. Tous les tests faits sur des hydrates de méthane sI donnent des résultats cohérents confirmant la sensible mais reproductible nature à haute température de cette conservation anomale. Des expériences avec des sauts de températures entre 250 et 268 K entérinent les taux relatifs préalablement mesurés dans les expériences isothermes et des tests à pression élevée sur les pores montrent que, tel que prévu, les taux de dissociation sont encore plus faibles si la pression est plus élevée. De façon surprenante, l'hydrate mixte de méthane–éthane n'exhibe pas un tel comportement lorsque rapidement dépressurisé à 268 K, même si ce mélange forme un hydrate thermodynamiquement stable à plus haute température et à plus basse pression que l'hydrate de méthane sI. Ces résultats, couplés avec l'imagerie SEM d'échantillons de matériel refroidis provenant d'une variété de tests de dissociation, supportent fortement nos arguments précédents qu'un effet d'écran de la glace produit par dissociation partielle le long des surfaces de grain de l'hydrate ne constitue pas le mécanisme premier de cette conservation anomale. Les mécanismes chimiques de base responsables de la conservation anomale demeurent difficiles à cerner, mais semblent être fondés plus sur les changement de texture ou de morphologie à l'intérieur de l'hydrate lui-même, plutôt que sur une répartition de composition ou un développement de la surface glacée.

[Traduit par la Rédaction]

1. Introduction and background

Gas clathrate hydrates are nonstoichiometric crystalline solids formed from the reaction of water and gas under certain conditions of relatively high pressure and low temperature. Three crystalline structures of gas hydrates have been identified in nature, structures I (sI), II (sII), and H, with different-sized lattice-cage diameters that accommodate different-sized gas molecules (see refs. 1 and 2 for further background). Hydrate deposits occur in polar regions as well as in continental margin sediments, and are most commonly found to contain a hydrocarbon gas mixture that is >99% methane and thus expected to be predominantly sI [2]. Natural sII gas hydrates have been recovered from the Gulf of Mexico and the Caspian Sea, and contain significant amounts of ethane and propane in addition to methane [3–5]. Structure H gas hydrate has also been observed in the Gulf of Mexico [6].

Over the past two decades, numerous observations of incomplete or delayed dissociation have been reported for a variety of gas-hydrate-bearing specimens of both natural and synthetic origin [7–13]. Such "self" preservation behavior occurs well above the equilibrium dissociation temperature of the gas hydrate but below the ice melting point. Quantitative comparison of the expected gas yields, extent of preservation, and comparison of preservation mechanisms among previously reported cases remains problematic, however. This is largely due to insufficient (or unavailable) information describing the precise stoichiometry, composition, or structure of the original hydrate, the difficulty in comparing pressure–temperature histories, the common presence of large fractions of H_2O ice as a secondary phase, or in the case of natural hydrate, the unknown extent of decomposition and alteration undergone by the hydrate during retrieval and handling procedures. In the cases cited above, the ice phase is typically estimated to account for at least 30 vol.% of the bulk sample, and in some cases upward of 90 vol.%. Shielding effects provided by either the large fraction of ice in the samples, or the formation of ice mantles on the surface of decomposing hydrate, have therefore been invoked as the principal

Fig. 1. Average rates at which sI methane hydrate samples reach 50% dissociation at 0.1 MPa and isothermal test conditions, following destabilization by rapid release of the sample pressure (modified from refs. 15 and 16 where the calculated rates were the inverse of time to 50% dissociation). Each solid circle represents a single sample depressurized and held at a constant temperature maintained by an external fluid bath. Open circles designate extrapolated rates for samples that never attained 50% dissociation over the isothermal portion of the test. The anomalous preservation regime between 242 and 271 K is characterized by markedly depressed dissociation rates that are orders of magnitude slower than those predicted by extrapolation of rates measured at lower temperatures (broken-line curve). The cause of the rate variation between 255 and 265 K is currently unknown, but is well defined and reproducible even within variable-temperature tests (see Fig. 2). Square symbols (connected by a dotted-broken line) designate experiments in which P_{CH_4} was maintained at 2 MPa, illustrating the improved preservation achieved by elevated pressure [23]. Diamonds show 0.1 MPa rapid depressurization tests conducted on sII methane–ethane hydrate, showing no comparable preservation behavior at 268 K. At the end of the isothermal portion of all experiments, samples were warmed through 273 K for collection and measurement of full gas yields.

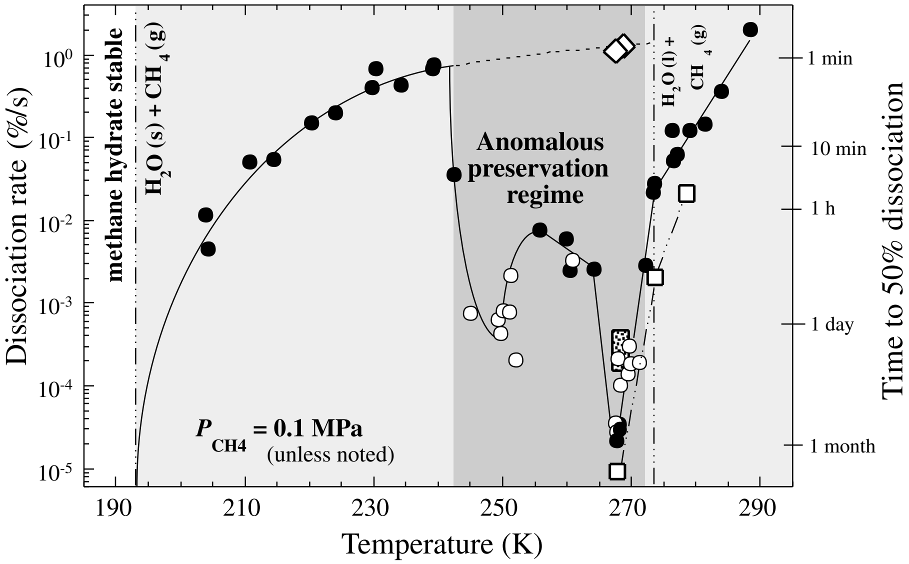

mechanism for incomplete dissociation. In a recent study reported by Takeya et al. [14], for example, time-resolved X-ray diffraction techniques were used to observe the dissociation of CH_4 hydrate crystals at <1 kPa methane pressure, at very low temperatures (168–189 K). They interpreted their observations to be in general agreement with an ice-shielding mechanism, concluding that the rate-limiting factor for the overall dissociation process is the diffusion of CH_4 gas through the thickening ice rind that develops around slowly dissociating methane hydrate crystals.

Previously, we reported on a pressure-release method by which methane hydrate can be reproducibly preserved in bulk at temperatures ranging 50 to 75 K above its stability limit of 193 K at 0.1 MPa [15–17]. Results from pressure-release tests identified three distinct thermal regimes with characteristic dissociation behavior (Fig. 1). Two span regions where dissociation rates increase monotonically with increasing temperature, as would be expected with increasing thermal oversteps of the equilibrium stability field. These regions occur at low temperature (195–240 K) where ice + CH_4 gas are decomposition products, and high temperature ($T > 273$ K) where liquid water + gas are products (see also ref. 18). Between these regions, at 242–271 K, exists a thermal regime in which dissociation rates diminish rapidly within seconds of depressurization, slowing to rates that are orders of magnitude lower than those predicted from the behavior observed in neighboring regimes (Fig. 1, broken-line curve). Methane hydrate dissociation rates were lowest in isothermal tests conducted at 5 ± 1° below the H_2O

melting point, where, in *all* tests, over 80 vol.% of the hydrate was preserved for at least 20 h after the pressure-release event. The amount of methane hydrate preserved by this method is well in excess of that reported in the earlier citations of self preservation, and appears to be the result of a mechanism different from ice encapsulation [15,17]. We note, however, that as warming of all preserved material through the melting point of ice induces rapid dissociation and release of all remaining gas, the presence of even small amounts of ice, or the mobility of molecular water at these temperatures, is somehow integral to the preservation effect.

Here, we report on recent gas-hydrate experiments that further explore the effects of temperature, pressure, and compositional variation on dissociation behavior, in an effort to better understand the underlying physical chemistry involved in anomalous and (or) self preservation. We report on rapid depressurization tests in which gas evolution was monitored while cycling sample temperature throughout the anomalous preservation regime, demonstraing a surprisingly reproducible thermal effect within this test region. Other depressurization tests were conducted in which sample pore pressure was reduced to that below the methane hydrate equilibrium curve but above 0.1 MPa, showing that, as expected, elevated sample pressure further reduces dissociation rates. To investigate grain morphology and the distribution of the dissociated ice product, we then imaged, by scanning electron microscopy (SEM), several samples from anomalous preservation tests taken to various states of completion. These images are also compared to those from largely decomposed samples that are known to consist predominantly of water ice. Lastly, we report on preliminary tests conducted on sII methane–ethane hydrate depressurized at 268 K, a hydrate phase that is stable at lower pressures and higher temperatures than sI methane hydrate. If ice shielding provided by either a mechanical or diffusion-limiting mechanism were in fact the primary cause of anomalous preservation, such sII hydrate might be expected to exhibit comparable or greater preservation behavior due to its increased range of stability, similar solubility characteristics of the hydrate guest phase, and larger guest-molecule size.

1.1. Experimental methods

Samples of polycrystalline methane hydrate (sI) and methane–ethane hydrate (sII) were grown in our laboratory by the warming and static conversion of small (200 μm) randomly-oriented grains of H_2O ice to grains of hydrate in a highly pressurized pure methane or methane–ethane (91:9 mol%) atmosphere [19,20]. This technique produces virtually pure methane hydrate of composition $CH_4 \cdot 5.89H_2O$ ("as-synthesized"), or methane–ethane hydrate of composition $(0.82CH_4 + 0.18C_2H_6) \cdot 5.67H_2O$. The methane–ethane system was chosen here for sII study because ethane is the second-most abundant hydrocarbon in natural gas hydrate, and because recent work reported by Subramanian et al. [21] demonstrated that these two sI hydrate formers in fact form sII when mixed to certain ratios. The composition of the methane–ethane source gas for this study was chosen to maximize the ethane content while still permitting adherence to our standard high-temperature high-pressure synthesis methods without condensing and unmixing the ethane phase.

Dissociation rates and sample stoichiometry were measured on more than 75 samples prepared in this manner. Each test monitored gas evolution from a dissociating sample by use of a custom-built gas flow meter and collection instrument connected directly to the synthesis chamber [22]. Most samples were tested immediately after synthesis to minimize any structural or compositional changes introduced by intermediate handling or cryogenic transfer. A typical 30 g sample of our material releases nearly 6 L of gas (at STP), all of which is collected in the flow meter chamber.

Two methods were used to destabilize samples: "temperature ramping" for precise measurement of stoichiometry and accurate prediction of gas yield, and "pressure release" for quickly accessing thermal regions where hydrate actively dissociates at 0.1 MPa. Both methods have been described previously [15,20]. Briefly, temperature ramping involves slow heating of pre-cooled samples at 0.1 MPa from 190 K through 273 K, at a rate of typically 8 K/h. Pressure release involves the initial venting of the sample pressure from post-synthesis conditions of elevated pressure (~30 MPa) to several MPa above the equilibrium curve, then thermal equilibration of the sample at a test temperature maintained by a large, external fluid bath (Fig. 5 in ref. 20). The remaining pressure is then vented to 0.1 MPa over a 6–10 s interval. The vent is then quickly closed while simultaneously opening the sample to the flow meter, allowing collection and flow measurement of the hydrate-forming gas [22]. Each data point in Fig. 1 represents a single pressure-release test performed at a single test temperature. In comparison, a second set of tests were conducted (Fig. 2) in which the external bath temperature was changed several times throughout a single experiment, to validate those measurements made previously on isothermal tests. All experiments were concluded by heating through 273 K to fully dissociate the preserved hydrate and to melt the accumulating ice product.

Sections from as-synthesized, temperature-ramping, and anomalously-preserved samples were imaged with a LEO 982 field emission SEM equipped with a Gatan Alto 2100 cryo-preparation and coating station, and cryo-imaging stage. Samples were first quenched in liquid nitrogen, transferred to the evacuated preparation chamber, then fractured with a cold blade to produce fresh surfaces for viewing. Most samples were coated with AuPd using a non-heat-emitting sputter head, then transferred directly to the SEM imaging stage. One sample was first imaged uncoated, then was coated mid-session and re-imaged to ensure that no surface damage was caused by the coating and transfer procedures. All samples were prepared and imaged at temperatures below 112 K, except for one sample that was briefly but actively dissociated at 195 K (in the SEM) for ice-phase identification. Imaging was conducted at 1–2 kV to minimize beam damage of the sample surface, and imaged sections of samples were typically relocated later in a session to monitor vacuum effects or any changes in surface topology over time. Most samples were prepared and analyzed in multiple sessions, by different researchers, to ensure imaging consistency.

2. Results and discussion

2.1. Temperature and pressure effects within the anomalous preservation region

Figure 2 shows the results from one of two methane hydrate samples that were first rapidly depressurized in the anomalous preservation regime, then cycled to different temperatures throughout this regime. These results clearly demonstrate that the temperature sensitivity of methane hydrate dissociation rates in the anomalous preservation regime (as mapped in Fig. 1) is a reproducible effect and not solely path dependent. The sample shown in Fig. 2 was initially depressurized and held at 268 K for over 23 h (Fig. 2A), during which it lost approximately 22% of its expected total gas yield (Figs. 2B and 2C). The sample was then cooled to 251 K and held for 4 h, during which time the dissociation rates increased measurably, causing the sample to lose an additional 6.8% of its gas. The sample was then warmed to 259 K and held for nearly 2 h, where rates increased again, causing the sample to lose an additional 8.7% of its gas. The sample was then rewarmed to its initial test temperature of 268 K and held for over 15 h, with rates dropping quickly to those measured during the initial 268 K step. After establishing this final isothermal measurement, the sample was heated through 273 K upon which it lost the remaining 50.5% of its gas (Figs. 2B and 2C). The final yield of the sample was 99.1% of the total expected gas yield, based on stoichiometry $CH_4 \cdot 5.89H_2O$.

Four thermocouples monitored the sample's internal temperature throughout the experiment, and an RTD monitored the external fluid bath temperature. For simplicity, only the centrally positioned sample thermocouple and bath RTD are plotted in Fig. 2. As shown in ref. 17, samples depressurized in the anomalous preservation region exhibit only brief temperature excursions from the external bath temperature immediately following pressure release, due to adiabatic cooling and minor dissociation, and during final heating through 273 K, due primarily to ice melting. Otherwise, the two track closely (Fig. 2A).

Preliminary tests investigating the effect of elevated pore pressure on methane hydrate dissociation also yielded self-consistent results, both within and above the anomalous preservation regime. Three samples that were depressurized to 2 MPa at isothermal test conditions of 268, 273, and 278 K (Fig. 1,

Fig. 2. Temperature-stepping experiment on methane hydrate, exploring the nonlinear temperature dependence of dissociation rates measured previously on individual (isothermal) samples tested *within* the anomalous preservation regime (see Fig. 1 data, 250–270 K). This sample was first depressurized and held at 268 K for 23 h (shown in (A)). Temperature was then quickly reduced and held at 251 K, then warmed and held at 259 K, then returned to 268 K (A). Methane-gas evolution was monitored throughout the experiment (B and C). The relative rates measured at the different temperature steps here match those measured previously in the individual tests shown in Fig. 1. After the second interval at 268 K, the sample was warmed through 273 K to dissociate the remaining hydrate. Symbols used in all panels are defined in (A).

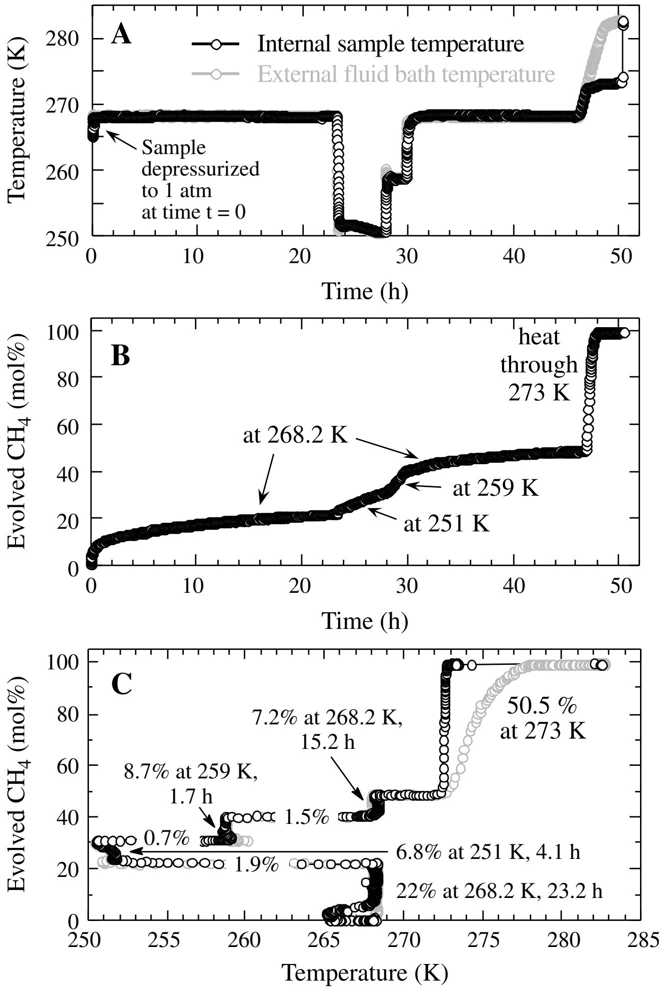

squares) all showed consistently slower dissociation rates than those depressurized to 0.1 MPa at the same test temperatures [23].

2.2. SEM imaging of as-grown, preserved, and dissociated methane hydrate

Figure 3 shows representative images of as-grown methane hydrate (Figs. 3A and 3B) versus anomalously-preserved material that was quenched 24 h after depressurization at 268 K, during which time it slowly lost 17% of its methane content (Figs. 3C and 3D). The as-grown material (30% porous) has a noticeably granular appearance and feel at the macroscopic level (Fig. 3A), but was found to be

Fig. 3. SEM images of fracture surfaces through as-synthesized (30% porous) methane hydrate, (A) and (B), and the upper central section of an anomalously-preserved methane hydrate sample, (C) and (D). The preserved sample was initially pressure-released and held at 268 K for 24 h, losing only 17% of it methane content prior to quenching for SEM observation. Although the as-synthesized material has a macroscopically granular appearance (A) reflecting its growth from fine-grained ice, it is shown to be densely recrystallized around large pores when viewed at higher resolution (B). In comparison, the anomalous preserved material (C) and (D) shows uniformly dense material with distinct textural changes along cavity walls (see text for further description).

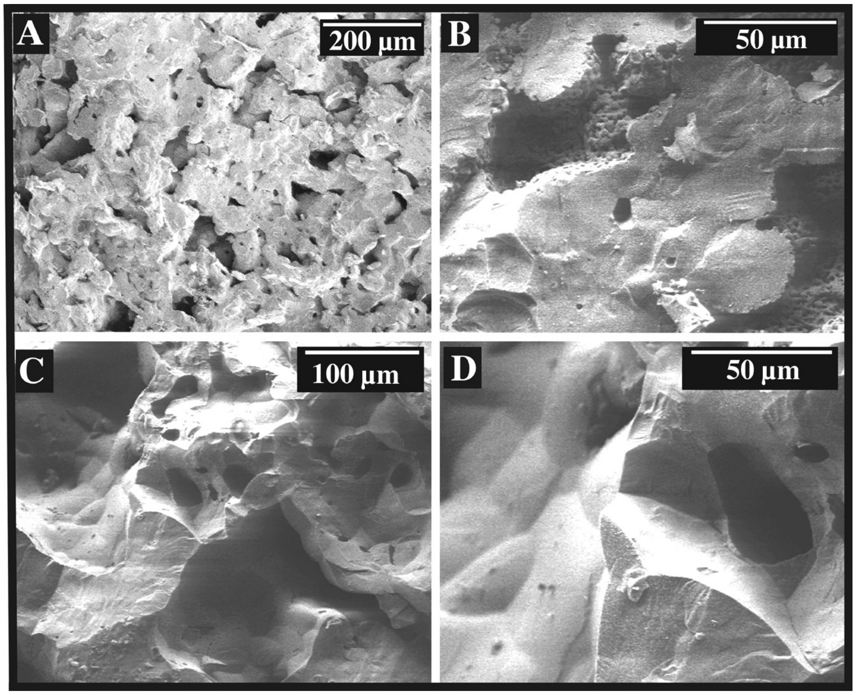

densely recrystallized around large cavities when viewed microscopically (Fig. 3B). Grain sizes in the as-grown methane hydrate product were typically found to be 20–40 μm. Cavity-lining textures and morphology varied considerably, sometimes displaying finely crystalline textures or sometimes pitted with a microporous appearance (Fig. 3B), while in other samples displaying highly faceted crystalline growth textures. Regardless of surface appearance, fractures through cavity edges revealed that the material is quite dense within several micrometres of the surface (Fig. 3B), suggesting that in some cases the microporous outer appearance might have been an artifact of the high-vacuum conditions within the SEM column. In comparison, anomalously-preserved samples show uniformly dense material with obvious textural changes at the granular scale (Figs. 3C and 3D). No isolated or near-spherical grains were observed in the preserved material, and no evidence was observed to indicate any apparent ice-rind development around individual hydrate grains (Figs. 3C and 3D).[2] Cavity-lining features were also observed to have recrystallized in all anomalously-preserved samples, developing smooth,

---

[2] In accordance with this, we note that one sample that was depressurized at 269 K and held isothermally for 90 min, during which time it lost 8 vol.% of its gas yield, was then quenched in liquid nitrogen and X-rayed for confirmation of its hydrate structure and bulk composition. The sample interior was found to be almost pure sI hydrate with $\leq$5 vol.% H_2O ice, indicating that (*i*) the preserved material appears to be predominantly methane hydrate and not a different structure, and (*ii*) the ice product formed during the early dissociation event does not occur on a grain-by-grain basis (i.e., developing as surface rinds, which should increase X-ray intensities by our powder diffraction methods) nor homogeously throughout the sample.

Fig. 4. SEM images of fracture surfaces through anomalously-preserved methane hydrate that was depressurized at 268 K and then held isothermally for over 400 h, during which time it slowly lost 57% of its methane content. This sample was then rapidly quenched for investigation of phase distribution and morphology. (A) and (B) from the upper/central (hydrate-rich) portion of the sample, show the dense material characteristic of anomalously-preserved samples (compare with Figs. 3C and 3D). (C) and (D) from the lower (ice-rich) section of the sample, show interspersed dense and porous material(s) (see text for further description).

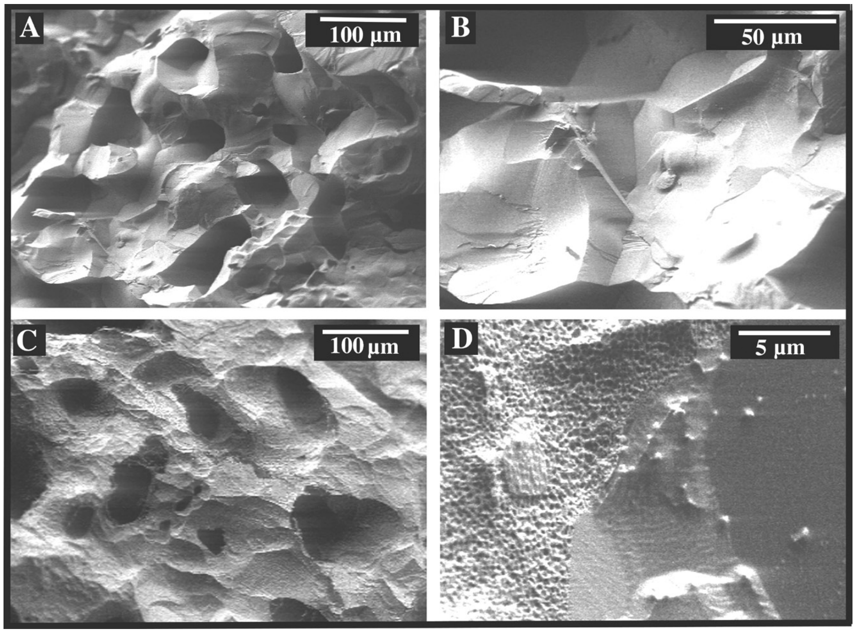

surface-minimization textures (Figs. 3C and 3D).

To investigate the appearance and distribution of ice in anomalously-preserved methane hydrate, a second sample was depressurized at 268 K to 0.1 MPa, then held isothermally for over 400 h before being quenched in liquid nitrogen for observation. This sample slowly lost 57% of its full methane content over the duration of the experiment. Macroscopic examination of the quenched sample showed that it had developed a grey and partially translucent ice-rich layer along its outer and lower surface of the sample, but that this layer did not fully encapsulate the sample. The upper and central portions of the sample remained porcelain-like, with a white, fine-grained, and competent texture characteristic of other anomalously-preserved samples that we have previously quenched for observation [15]. Two sections of this sample were imaged by SEM, one from the top-central (hydrate-rich) portion of the sample, the other from the lower central (mixed ice + hydrate) section of the sample (Fig. 4). The upper portion of the sample showed the same densely-recrystallized texture as that displayed by the 17% dissociated sample (compare Figs. 4A and 4B with Figs. 3C and 3D). In contrast, the lower, ice-rich portion of the sample exhibited distinct and blocky sections of dense material interspersed with more porous and in some places frothy-appearing material (Figs. 4C and 4D). Although ice and hydrate can be extremely difficult to differentiate by SEM, the textures observed in this sample suggest that when ice occurs directly as a hydrate-dissociation product (i.e., in samples dissociated at $T < 273$ K where ice, not liquid water, is the dissociation product), it has a markedly aerated appearance.

For further inquiry into the appearance of ice as it occurs as a hydrate decomposition product, two other ice-rich samples were imaged by SEM. The first, a temperature-ramping sample that was quenched in liquid nitrogen after the main dissociation event (i.e. but not warmed through 273 K to release its residual 3–5% methane hydrate) is shown in Figs. 5A and 5B. The second, a sample of

Fig. 5. SEM images of ice, as it occurs as a dissociation product of methane hydrate decomposed at $T < 273$ K. (A) and (B) show low- and high-resolution images of a temperature-ramping experiment (see text) that was quenched from 225 to 77 K following the main dissociation event. This sample is ~96% ice, with the residual methane hydrate dispersed within it. (C) and (D) show low- and high-resolution images of a methane hydrate sample (as-synthesized) that was briefly warmed above 195 K in the SEM until visible surface dissociation occurred, then quickly re-cooled for imaging. Both samples show that ice exhibits a porous, frothy appearance when it occurs as a product of low-temperature hydrate breakdown.

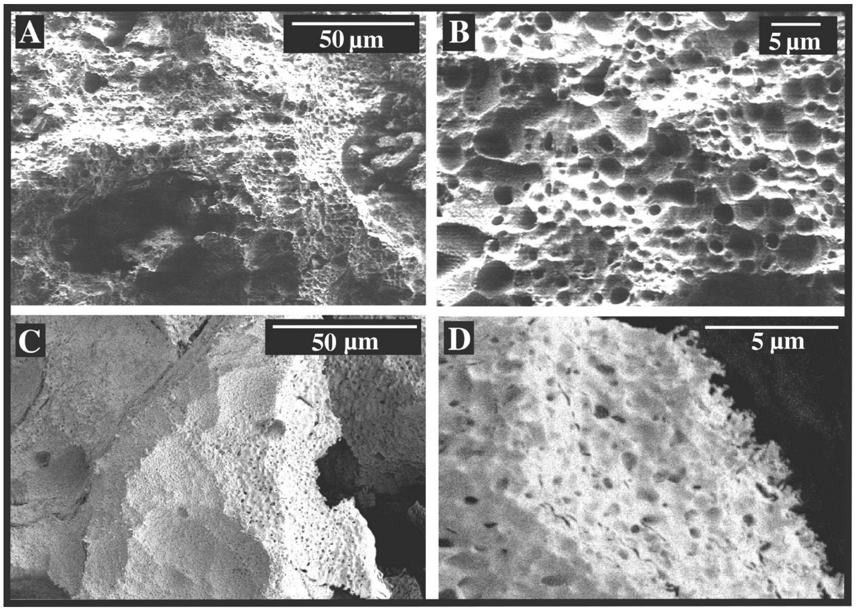

as-grown methane hydrate that was briefly warmed to 195 K in the SEM until its surface was observed to actively dissociate to ice, is shown in Figs. 5C and 5D. Both samples exhibit distinctly porous and frothy textures similar to that which we attribute to the ice development in Fig. 4. We note that these samples have undergone different thermal histories, but the strong similarities in textural appearance among these three samples that all contain significant ice fractions argue in favor of this interpretation.

2.3. Stability of sII methane–ethane hydrate

Samples of sII methane–ethane hydrate were tested first in temperature-ramping dissociation tests, to observe the onset of dissociation at 0.1 MPa and to measure the full gas yield of the as-grown material (Fig. 6A). As expected, the sII hydrate is stable to warmer temperatures than is sI methane hydrate, and has nearly ideal stoichiometry.

Two samples of sII methane–ethane hydrate were then tested in pressure-release tests at 268 K, using the same protocols as those used in sI methane hydrate tests. Both sII samples behaved identically, showing no preservation effect. Instead, approximately 96% of both samples dissociated within 3 min, with the remaining gas released upon subsequent warming through 273 K. Figure 6B compares one of these sII samples to a 268 K test on sI methane hydrate, illustrating the dramatic difference in dissociation behavior. Interestingly, the sII hydrate dissociated at a rate close to that shown by the broken-line curve in Fig. 1 (“predicted” behavior in the total absence of anomalous preservation).

2.4. The ice-shielding mechanism

We previously compared in detail hydrate self-preservation effects observed in other studies to our own measurements [15,17]. Ice encapsulation of the residual hydrate may well serve as the primary

Fig. 6. Comparison of dissociation behavior between sI methane hydrate (open symbols) and sII methane–ethane hydrate (solid symbols) when destabilized by either slow warming above the 0.1 MPa dissociation temperature ("temperature ramping") as shown in (A), or by rapid depressurization at 268 K, shown in (B). In (B), samples were pressure-released at time $t = 0.1$ h. (Note that time is plotted logarithmically.) Although the sII hydrate is stable to higher temperatures and lower pressures than sI methane hydrate, it exhibits no comparable anomalous preservation behavior at 268 K. While 96% of the sII hydrate dissociated within 0.07 h of the pressure release, only 40% of the sI hydrate dissociated within 160 h of the pressure release. In another experiment (not shown), 50% of the methane hydrate persisted after 410 h. The temperature of the sII hydrate plummeted 40° during its rapid dissociation, in contrast to the brief and minor depression exhibited by methane hydrate (see Fig. 2A). Following the isothermal portion of both tests, samples were heated through 273 K to dissociate the remaining hydrate (shaded region). The evolved gas scale in (B) is normalized such that 100% represents ideal stoichiometry for the two different structures.

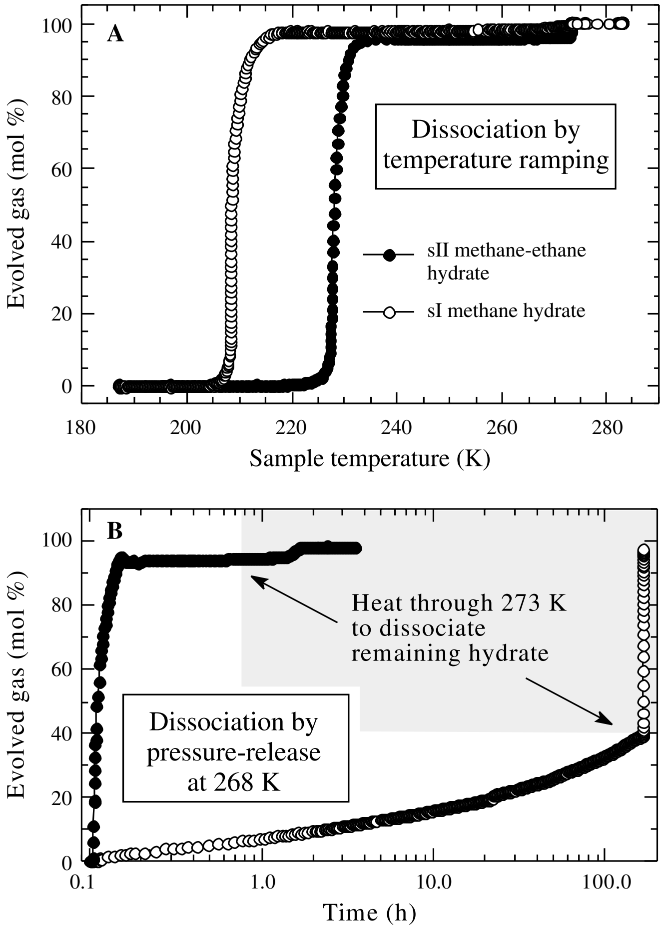

mechanism for preservation of the small amounts of hydrate observed in our temperature-ramping tests as well as in pressure-release tests conducted at 195–240 K. This hypothesis is substantiated by the observation that warming such samples into the "premelting" zone of ice increases the release rate of the residual gas within them (detailed in Fig. 2A inset of ref. 15). The upper extent of the premelting zone, however, includes the specific temperature range at which anomalous preservation of methane hydrate is most pronounced. We therefore speculate that while preservation of the residual hydrate in both the ramping tests and the low-temperature depressurization tests is related to the progressive ice development around dissociating hydrate, anomalous preservation appears to be a different process, or at least one that is not due primarily to a mechanical or diffusion-rate-limiting encapsulation mechanism. The complex temperature dependence of methane hydrate dissociation behavior (Figs. 1 and 2) further supports this argument, as does the fact that the methane equilibrium gas pressure required to stabilize methane hydrate in the upper reaches of the anomalous preservation regime is more than double that required to stabilize hydrate in lower temperature regions. We also note that the most "successful" preservation of bulk hydrate is observed at the highest temperatures of the ice premelting zone, where the plastic strength of ice is at its lowest, and where diffusion rates of methane through ice should increase.

Stress analysis modeling of a spherical ice-rind/hydrate-core geometry also indicates that ordinary hexagonal water ice is mechanically incapable of containing a sufficiently high pressure of free methane gas to stabilize methane hydrate within the anomalous preservation thermal regime. Published details in the literature of the postulated ice-surface-layer model are sketchy. Here, we assume spherical geometry since it offers a conservative and lower boundary calculation of stresses. We also assume for calculation purposes that the ice layer is a uniform, continuous, and impermeable shell, serving effectively as a barrier to gas flow across it. If we assume that the gas pressure inside the shell is maintained at or above the minimum hydrate stability pressure at the ambient temperature, then stresses in the shell can be calculated from force balance considerations. At the optimal temperatures for anomalous preservation, 267–270 K (Fig. 1), the minimum methane pressure for hydrate stability is 2.1–2.4 MPa. Assuming methane gas pressure outside the shell is 0.1 MPa, the pressure difference across the shell is 2.0–2.3 MPa. For anomalous preservation, we estimate the wall thickness of the presumed ice shell for 80–90% preservation to be 10 μm or less for hydrate grains of average radius of 125 μm; the inner radius of the shell would therefore be 115 μm. For the case of self preservation, the ice wall thickness would be approximately 80 μm and the inner radius 45 μm. At the maximum stresses generated in the ice shell, however, the resultant strain rate for the ice phase (see, for example, ref. 24) for the anomalous preservation case would be implausibly high ($>10^{-2}$ s^{-1}). In the case of self preservation, the strain rate would still be quite rapid ($>10^{-6}$ s^{-1}), but conceivable. We note that the hydrate grain diameters used in these calculations are based on the size of the granular ice starting material from which the hydrate was initially grown, and in fact SEM imaging shows that substantial recrystallization and grain-size reduction takes place during synthesis (Figs. 2A and 2B). Nevertheless, model calculations scaled to smaller grain sizes (20–50 μm) yield similar qualitative results. Alternatively, it could be argued that perhaps the low solubility of methane in ice rinds maintains a sufficiently high methane fugacity to stabilize hydrate cores. This argument does not, however, readily explain why the residual 3–8 vol.% hydrate in temperature-ramping tests or low-temperature depressurization tests begins to *release* gas over the very temperatures where anomalous preservation is most pronounced.

The experimental results reported here are also inconsistent with an ice encapsulation model as providing the primary mechanism for anomalous preservation. The lack of preservation observed in sII methane–ethane-hydrate experiments, for instance, shows that ice-rind development does not preserve sII methane–ethane-gas hydrate at 268 K, even though the equilibrium pressure required to stabilize such sII hydrate is roughly half that of sI methane hydrate, and even though this sII hydrate contains a larger diameter guest molecule that should hinder its diffusion through ice. Furthermore, SEM imaging of anomalously-preserved methane hydrate samples shows no obvious evidence of ice encapsulation of hydrate on either the granular- or sample-wide scale, even in those samples that were preserved for several weeks at 268 K and that dissociated by 50–60%. SEM imaging also revealed no evidence to validate the geometrical modeling of the dissociating material by a simple shrinking core model. Instead, the images show that extensive recrystallization or other textural changes occur within those samples, so that the preserved material is extremely dense and anneals to form smooth, minimal-surface grain textures along pore walls. Based on these measurements and observations, the ice barrier theory does not readily explain the well-defined but extremely nonlinear temperature dependence of methane hydrate anomalous preservation behavior.

3. Conclusions

While the mechanism of anomalous preservation remains elusive, the phenomenon is highly reproducible and experimentally well-resolved. Ice-shielding is a plausible explanation for self preservation of residual gas hydrate ($<8\%$) in temperature-ramping tests and in low-temperature rapid-depressurization tests, but does not adequately explain anomalous preservation of methane hydrate at 242–271 K. The complex and extremely nonlinear temperature-dependence of methane hydrate dissociation behavior, the absence of ice-rind development in preserved samples, and the utter lack of comparable preservation behavior in sII methane–ethane hydrate, all strongly suggest that a different preservation mechanism is involved. We speculate that it may be one that is inherent to the methane hydrate material itself.

Anomalous preservation of methane hydrate, produced by pressure-release at temperatures just below the H_2O melting point, offers novel applications for the retrieval of naturally-occurring methane hydrate and for the temporary low-pressure transport or storage of manufactured or collected methane hydrate. It is also an effect that has not been carefully considered for stability issues involving deep-water drilling into or through methane hydrate-bearing sediments, or models of sea-floor stability where rapid pressure-release along fault vents may occur. It is now clear, however, that this effect cannot necessarily be exploited for applications involving all compositions or structures of gas hydrate. Further investigation of the physical chemistry underlying anomalous preservation is clearly required for practical utilization or modeling of its effects.

Acknowledgements

We thank J. Pinkston and R. Oscarson of the USGS for their technical help in the laboratory and SEM facility, and Pauline Yu of the USDA for imaging the sample shown in Figs. 5C and 5D. We also thank W. Waite (USGS), M. Helgerud (Exxon Corp.), and two anonymous reviewers for their comments to this manuscript. This work was supported under the auspices of the USGS and by the Methane Hydrate R& D Program of the US DOE, National Energy and Technology Laboratory.

References

1. E. Sloan. Clathrate hydrates of natural gases. 2nd ed. Marcel Dekker, New York. 1998.
2. K. Kvenvolden. *In* Natural gas hydrate: in oceanic and polar subaerial environments. *Edited by* M. Max. Kluwer, Dordrecht. 2000. Chap. 2. pp. 9–16.
3. J. Brooks, M. Kennicutt, R. Fay, and T. McDonald. Science (Washington), **225**, 409 (1984).
4. A. Yefremova and N. Gritchina. Geol. Nefti Gaza, **2**, 3 (1981).
5. G. Ginsburg, R. Guseinov, A. Dadashev et al. Izv. Akad. Nauk, Ser. Geol. **7**, 5 (1992).
6. R. Sassen and I. MacDonald. Org. Geochem. **22**, 1029 (1994).
7. D. Davidson, S. Garg, S. Gough, Y. Handa, C. Ratcliffe, J. Ripmeester, and J. Tse. Geochim. Cosmochim. Acta, **50**, 619 (1986).
8. Y. Handa. J. Chem. Thermodyn. **18**, 891 (1986).
9. V. Yakushev and V. Istomin. *In* Physics and chemistry of ice. *Edited by* N. Maeno and T. Hondoh. Hokkaido University Press, Sapporo. 1992. pp. 136–139.
10. Y. Handa and D. Stupin. J. Phys. Chem. **96**, 8599 (1992).
11. J. Gudmundsson, M. Parlaktuna, and A. Khokhar. SPE Prod. Fac. (1994). p. 69.
12. S. Dallimore and T. Collett. Geology, **23**(6), 527 (1995).
13. O. Levik and J. Gudmundsson. Ann. N.Y. Acad. Sci. **912**, 602 (2000).
14. S. Takeya, W. Shimada, Y. Kamata, T. Ebinuma, T. Uchida, J. Nagao, and H. Narita. J. Phys. Chem. A, **105**, 9756 (2001).
15. L. Stern, S. Circone, S. Kirby, and W. Durham. J. Phys. Chem. B, **105**(9), 1756 (2001).
16. L. Stern, S. Circone, S. Kirby, and W. Durham. Energy Fuels, **15**(2), 499 (2001).
17. L. Stern, S. Circone, S. Kirby, and W. Durham. J. Phys. Chem. B, **106**(1), 228 (2002).
18. S. Circone, L. Stern, S. Kirby, J. Pinkston, and W. Durham. Ann. N.Y. Acad. Sci. **912**, 544 (2000).
19. L. Stern, S. Kirby, and W. Durham. Science (Washington), **273**, 1843 (1996).

20. L. Stern, S. Kirby, W. Durham, S. Circone, and W. Waite. *In* Natural gas hydrate: in oceanic and polar subaerial environments. *Edited by* M. Max. Kluwer, Dordrecht. 2000. Chap. 25. pp. 323–349.
21. S. Subramanian, R. Kini, S. Dec, and E. Sloan. Ann. N.Y. Acad. Sci. **912**, 873 (2000).
22. S. Circone, S. Kirby, J. Pinkston, and L. Stern. Rev. Sci. Instrum. **72**(6), 2709 (2001).
23. S. Circone, S. Kirby, J. Pinkston, and L. Stern. EOS Trans. Am. Geophys. Union, **83**, F777 (2002).
24. W. Durham and L. Stern. Annu. Rev. Earth Planet. Sci. **29**, 295 (2001).